A reconsideration of the safety of piled bridge foundations in liquefiable soils

S. Bhattacharya, S.P.G. Madabhushi, M.D. Bolton, S.K. Haigh and K. Soga

Cambridge Geotechnical Research Group, Schofield Centre, University of Cambridge (U.K).

ABSTRACT

Collapse of piled foundations in liquefiable soil has been observed in the majority of recent strong earthquakes despite the fact that a large margin of safety is employed in their design. This paper critically reviews the current understanding of pile failure in liquefiable deposits with special reference to JRA (1996) code. Critical remarks have been made on the current understanding of pile failure using the well-known and well-documented failure of the Showa Bridge. It has been shown that the current understanding cannot explain some observations of pile failure. The current method of pile design under earthquake loading is based on a bending mechanism where the inertia and slope movement (lateral spreading) induce bending in the pile, and where axial load effects are ignored. An alternative mechanism of pile failure in liquefiable deposits has been proposed. This mechanism, based on pile buckling, is formulated by back analysing fifteen case histories of pile foundation performance during past earthquakes and verified using dynamic centrifuge modelling. The practical implications of the research have been highlighted.

Key words: Pile failure, Buckling, Case histories, Showa Bridge, JRA (1996) code, Lateral spreading, Liquefaction, Effective length.

INTRODUCTION

Structural failure of piles passing through liquefiable soils has been observed in many of the recent strong earthquakes. This suggests that the bending moments or shear forces that are experienced by the piles exceed those predicted by their design methods (or codes of practice). The Japanese Road Association Code, (JRA, 1996) does consider the effects of soil liquefaction, which it assumes are related to the drag on the piles caused by lateral spreading of the soil, as in National Research Council (NRC, 1985), Hamada (1992a, 1992b, 2000), Ishihara (1993, 1997), Finn and Thavaraj (2001), Finn and Fujita (2002), Abdoun and Dobry (2002). All current design codes apparently provide a high margin of safety (using partial safety factors on load, material stress which increases the overall safety factor), yet occurrences of pile failure due to liquefaction are abundant. This implies that the actual moments or shear forces experienced by the pile are many times higher than the predictions. It must be concluded that the current design methods may not be consistent with the physical processes or mechanisms that govern liquefaction-induced failure. This paper investigates buckling as an alternative mechanism for pile failure due to soil liquefaction. Reference is made, as a case study, to the well-known failure of the Showa Bridge, which is evaluated to be safe according to the JRA (1996).

CURRENT UNDERSTANDING AND JRA (1996)

Chapter 7 (page 77) of JRA (1996) begins with a general introduction on seismic design of foundations which summarises the possible consequences of soil liquefaction as follows:

"*When soil liquefies, structures with an apparent high specific gravity subside, structures with an apparent low specific gravity rise, structures which bear against soil are pushed forward by the increase in soil pressure, while foundations and other structures to provide horizontal resistance are displaced as their resistance strength falls sharply. Additionally, liquefaction of ground near a shoreline or on a grade induces lateral spreading*".

This paper points out that the soil surrounding slender piles is required to provide horizontal resistance to prevent lateral buckling, and that this resistance can fall to near zero due to soil liquefaction. However, JRA (1996) chapter 7 specifies no design checks against buckling. The required calculations include the possibility of lateral spreading, as suggested in the second sentence of the quote above and loss of bearing capacity as suggested in the first sentence above.

The current understanding of pile failure (as noted in the literature and design codes) is as follows: Soil liquefies, losing its shear strength, causing it to flow taking with it any overlying non-liquefied crust. These soil layers drag the pile with them, causing a bending failure. This is often referred to as failure due to lateral spreading. In terms of soil-pile interaction, the current

mechanism of failure assumes that the *soil pushes the pile*. The Japanese Highway code of practice (JRA 1996) has incorporated this concept as shown in Figure 1. The code advises practising engineers to design piles against bending failure assuming that the non-liquefied crust offers passive earth pressure to the pile and the liquefied soil offers 30% of total overburden pressure. Yokoyama et al. (1997) reports that this code was formulated by back analysing a few piled bridge foundations of the Hanshin expressway that were not seriously damaged following the 1995 Kobe earthquake.

Inertia of the superstructure can also induce bending moments in the pile. In this regard JRA (1996) in page 78 says:

"*In a case where the effects of lateral spreading are accounted, the effect of lateral spreading shall be provided as horizontal force to study the seismic performance of the foundation. But in this case, it shall not be necessary to simultaneously account for the inertia force produced by the weight of the structure"*.

Ishihara (1997) illustrates the background for such a clause in the code. He notes that, the onset of liquefaction takes place approximately at the same time when the peak acceleration occurs in the course of seismic load application having an irregular time history. He argues that the seismic motion has already passed the peak and shaking may be persistent with lesser intensity and therefore, the inertia force transmitted from the superstructure will be insignificant. Hamada (2000) in the 12th World Congress on Earthquake Engineering concludes that permanent displacement of non-liquefied soil overlying the liquefied soil is a governing factor for pile damage. Similar conclusion has also been reached by Berrill et al. (2001).

Other codes of practice such as the USA code (NEHRP 2000), Eurocode 8, part 5 (1998) and Indian code (IS 1893, 2002) also focus on the bending strength of the pile. Based on the assumption that lateral spreading is the cause of pile failure, research work into this pile failure mechanism has been conduced by various researchers, such as Sato et al (2001), Takahashi et al. (2002), Haigh (2002), Tokimatsu et al (2001), Berrill et al (2001), Ramos et al (2000). Sato et al., (2001) through stress cell measurements concludes that the forces predicted by JRA (1996) are over-conservative. The centrifuge test results of Haigh (2002) shows that pressure distribution of JRA (1996) is un-conservative in transient phase but gives reasonable predictions at residual stage.

This hypothesis of pile failure simply treats piles as beam elements and assumes that the pile remains in stable equilibrium (i.e. vibrates back and forth and does not move unidirectionally as in the case of buckling instability) during the period of liquefaction and before the onset of lateral spreading. The effect of axial load as soil liquefies is ignored in this hypothesis. In other words, the hypothesis ignores the structural nature of the pile as explained in the next section.

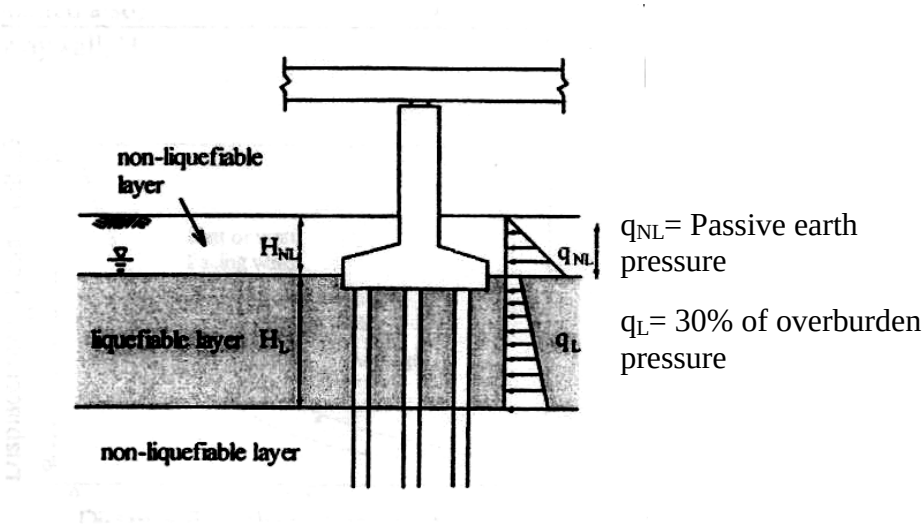

Figure 1: JRA (1996) code of practice showing the idealisation for seismic design of bridge foundation.

PILE BUCKLING

Structural engineers would often have to regard piles as slender columns were it not be lateral support from the surrounding soil. Generally, as the length of the pile increases, the allowable load on the pile increases primarily due to the additional shaft friction but the buckling load (if the pile were laterally *unsupported* by soil) decreases inversely with the square of its length following Euler's formula. Figure 2 shows a typical plot for the variation of allowable load (P) and buckling load (P_{cr}) of a pile (if *unsupported*) against length of the pile. The pile in the above example has a diameter of 300mm (typical pile dimension in 1964 Japan) and is passing through a typical liquefied soil. The allowable load (P) is estimated based on conventional procedures with no allowance for liquefaction. Structural engineers generally demand a factor of safety of at least 3 against linear elastic buckling to allow for eccentricities, imperfections and reduction of stiffness due to yielding. Thus, if *unsupported* over a length of 10m or more, such columns could fail due to buckling instability and not due to crushing of the material. During earthquake-induced liquefaction, the soil surrounding the pile loses its effective confining stress and can no longer offer sufficient support to it. The pile, if sufficiently slender, may now act as an unsupported column prone to axial instability. The instability may cause it to buckle sideways in the direction of least elastic bending stiffness under the action of axial load, eventually causing a plastic hinge, see for example Bhattacharya et al (2002, 2003), Bhattacharya (2003), Bhattacharya and Bolton (2004a, 2004b). Figure 3 shows instability of a frame supported on slender columns, as load is increased. At a particular load the frame becomes unstable and this is often termed as Euler's critical load (P_{cr}). Imperfections, such as lateral loads or out-of-line straightness will increase lateral deflections,

which in turn induces plasticity in the strut and reduces the buckling load, promoting a more rapid collapse.

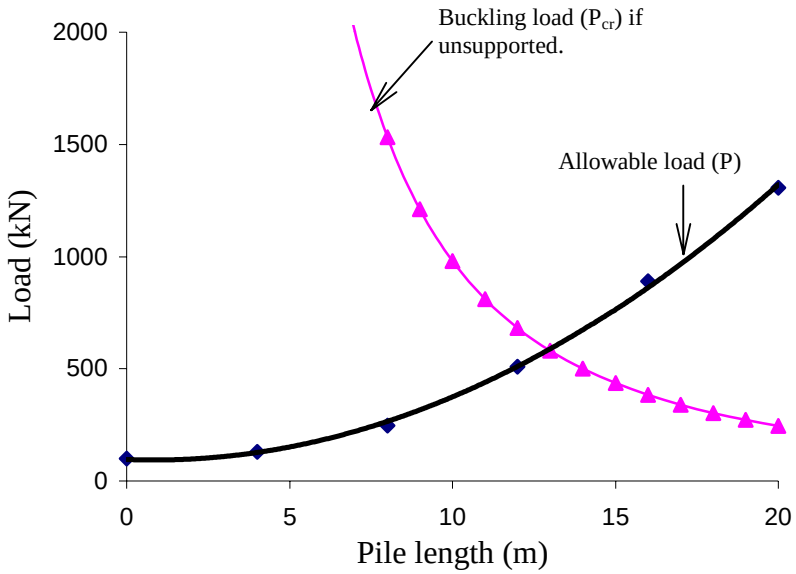

Fig. 2: Allowable load and buckling load (if unsupported) of a typical pile.

Figure 3: Instability test with slender columns.

STUDY OF CASE HISTORIES

In this study, fifteen reported cases of pile foundation performance during earthquake-induced liquefaction has been studied and analysed as listed in Table 1. Six of the piled foundations were found to survive while the others suffered severe damage (Bhattacharya, 2002 and Bhattacharya et al., 2002). The parameters r_{min} (minimum radius of gyration) and L_{eff} (effective length of the pile in liquefiable region) are introduced to analyse the piles. The definitions of the parameters are given below.

1. r_{min} : The minimum radius of gyration of the pile section about any axis of bending (m).This parameter can represent piles of any shape (square, tubular or circular) and is used by structural engineers for studying buckling instability and is given by Equation 1.

$$r_{min} = \sqrt{\frac{I}{A}} \qquad (1)$$

where:

I = second moment area of the pile section about the weakest axis (m^4).

A= area of the pile section (m^2).

For solid circular piles r_{min} is 0.25 times the diameter of the pile and for tubular piles r_{min} is approximately 0.35 times the outside diameter of the pile.

2. L_{eff} = Effective length of the pile in the liquefiable region. The definition of effective length has been adopted from column stability theory. This parameter depends on the depth of liquefiable region (L_0) and the boundary condition of the pile as shown in Figure 4(a). The different boundary conditions of pile tip and pile head can be adopted as shown in Figure 4(b). L_{eff} is also familiar as the "Euler's buckling length" of a strut pinned at both ends. In practice, designers may prefer to extend the effective length by a few diameters to account for imperfect fixity in the non-liquefying layer; see Fleming et al. (1992).

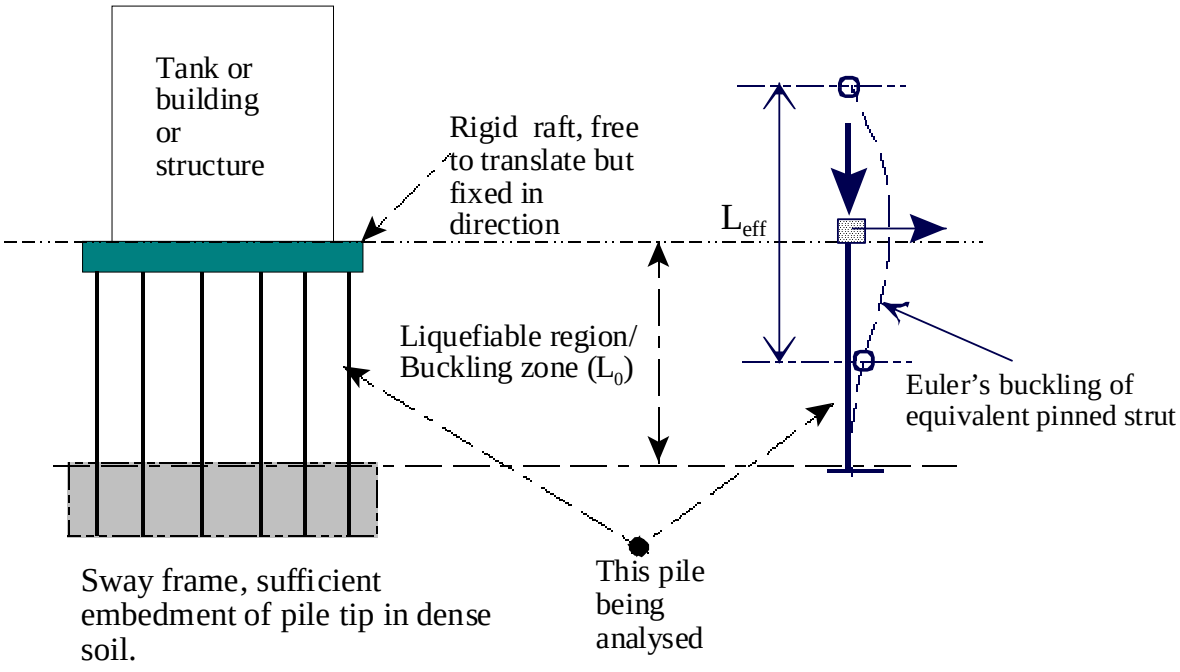

Figure 4 (a): Effective length of pile in case of large raft.

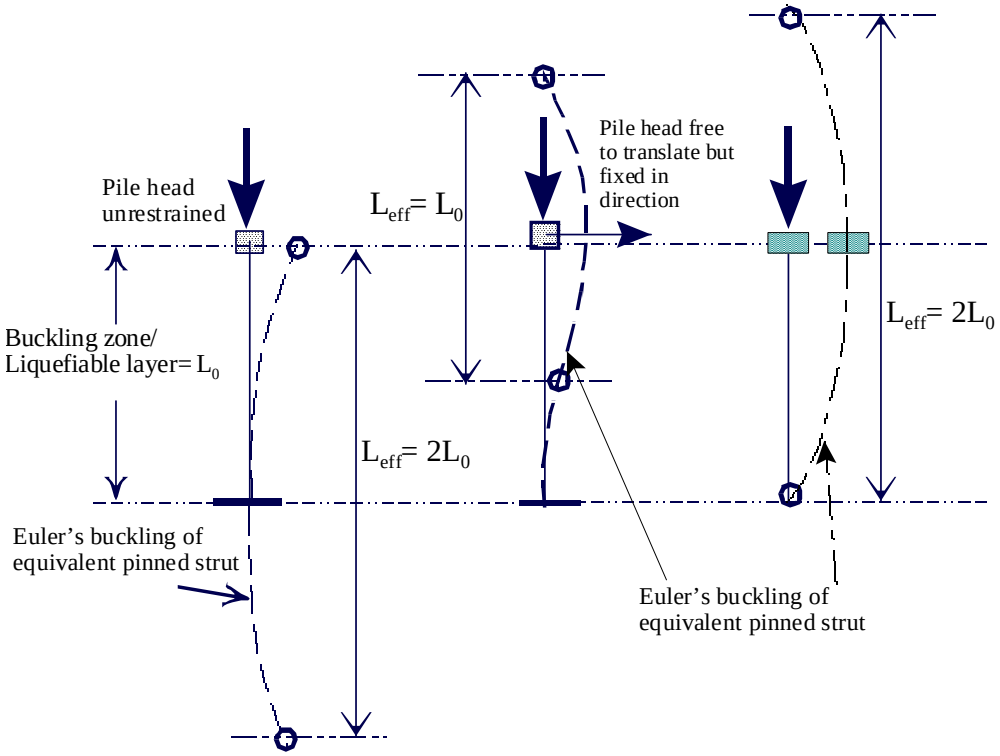

Figure 4 (b): Concept of effective length

Table 1: Summary of case histories.

ID in Fig 5	Case History and Reference	Pile section/ type	L_0^* (m)	L_{eff} (m)	r_{min} (m)
A	10 storey-Hokuriku building, Hamada (1992a)	0.4m dia RCC	5	5	0.1
B	Landing bridge, Berrill et al (2001)	0.4m square PSC	4	2	0.12
C	14 storey building, Tokimatsu et al (1996)	2.5m dia RCC	12.2	12.2	0.63
D	Hanshin expressway pier, Ishihara (1997)	1.5m dia RCC	15	15	0.38
E	LPG tank 101, Ishihara (1997)	1.1m dia RCC	15	15	0.28
F	Kobe Shimim hospital, Soga (1997)	0.66m dia steel tube	6.2	6.2	0.23
G	N.H.K building, Hamada (1992a)	0.35m dia RCC	10	20	0.09
H	NFCH building. Hamada (1992a)	0.35m dia RCC hollow	8	16	0.10
I	Yachiyo Bridge Hamada (1992a)	0.3m dia RCC	8	16	0.08
J	Gaiko Ware House, Hamada (1992b)	0.6m dia PSC hollow	14	28	0.16
K	4 storey fire house, Tokimatsu et al (1996)	0.4m dia PSC	18	18	0.10
L	3 storied building at Kobe university, Tokimatsu et al (1998)	0.4m dia PSC	16	16	0.12
M	Elevated port liner railway, Soga (1997)	0.6m dia RCC	12	12	0.15
N	LPG tank –106,107 Ishihara (1997)	0.3m dia RCC hollow.	15	15	0.08
O	Showa bridge, Hamada (1992a)	0.6m dia steel tube.	19	38	0.21

L_0^* = Length of pile in liquefiable layer/buckling zone, see Figure 4(b).

The ratio L_{eff}/r_{min} is termed as slenderness ratio of pile in liquefiable region. Figure 5 plots the L_{eff} against the r_{min} of the pile section with identification of their performance during earthquakes. A line representing a slenderness ratio (L_{eff}/r_{min}) of 50 is drawn and it distinguishes

poor performance piles from the good ones. This line is of some significance in structural engineering, as it is often used to distinguish between “long” and “short” columns. Columns having slenderness ratios below 50 are expected to fail in crushing whereas those above 50 are expected to fail in buckling instability. Thus, the analysis suggests that pile failure in liquefied soils is similar in some ways to the failure of long columns in air. The lateral support offered to the pile by the soil prior to the earthquake is removed during liquefaction.

It has been hypothesised based on the above study that a pile can become unstable under the action of axial load provided the slenderness ratio of the pile in the unsupported zone exceeds a critical value. It may not be necessary to invoke lateral spreading of the soil to cause a pile to collapse and piles can collapse before lateral spreading starts, once the soil has liquefied.

The plot of P (allowable load of the pile obtained from conventional procedure with no allowance for liquefaction) and P_{cr} (buckling load, if *unsupported*) for the piles that failed in Figure 5 can be seen in Figure 6 following Bhattacharya et al (2002). It may be observed from the plot that the piles that failed had (P/P_{cr}) ratio between 0.5 and 1. On the other hand, the analysis of the case histories (see Bhattacharya et al. 2002) shows that the piles that survived the earthquake in laterally spreading soil had (P/P_{cr}) ratio below 0.1.

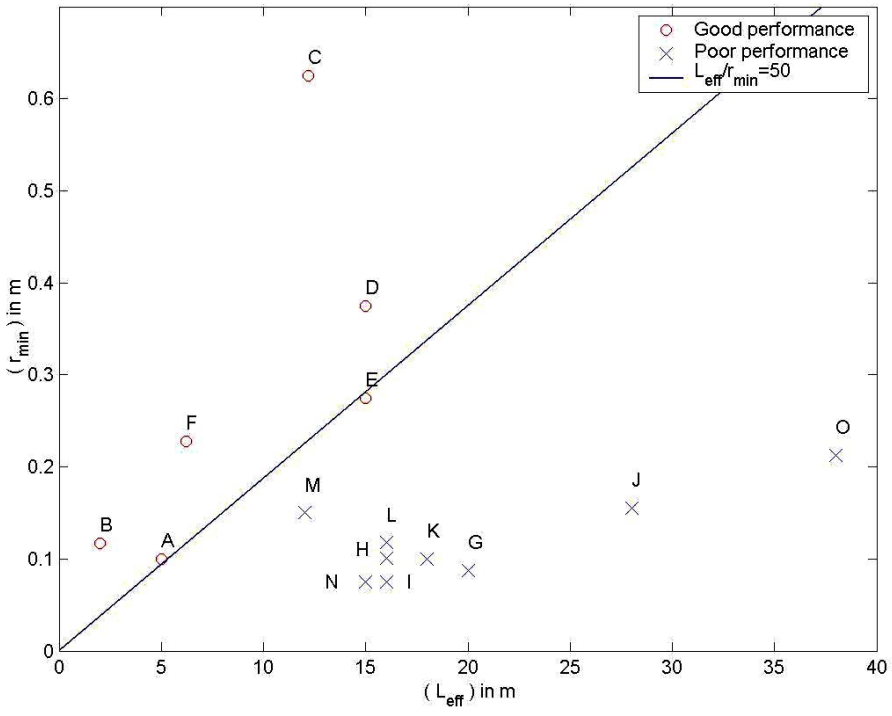

Figure 5: L_{eff} versus r_{min} for piles studied.

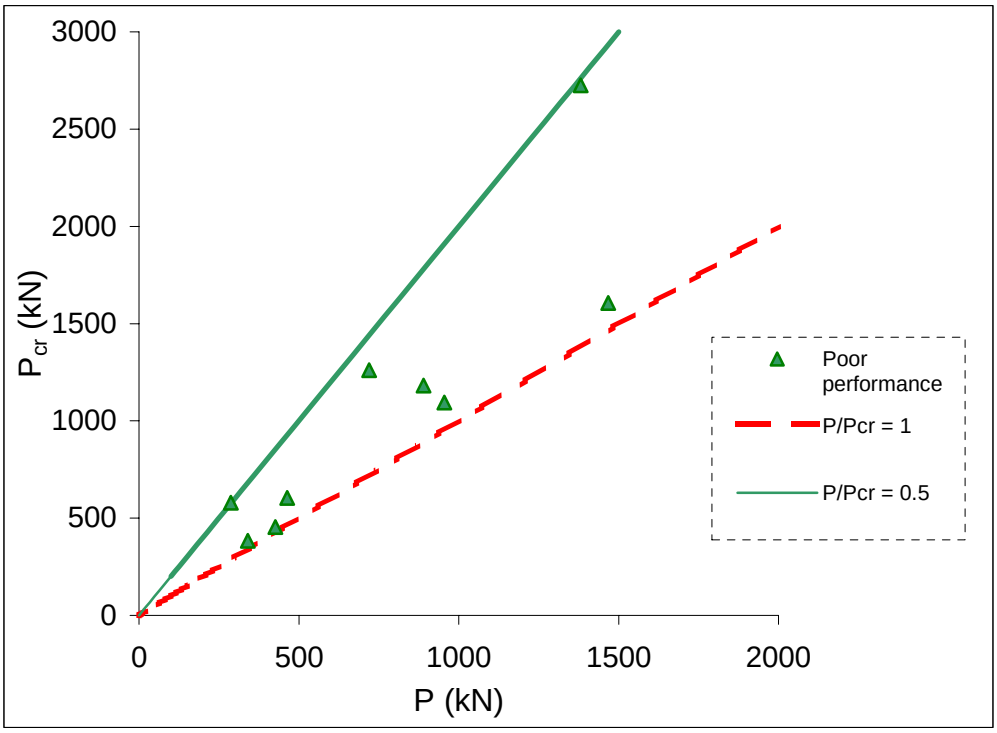

Figure 6: Plot of P and P_{cr} of the poor performance piles in Figure 5

PILE BUCKLING IN A CENTRIFUGE TEST

Dynamic centrifuge tests were carried out at Cambridge Geotechnical Research Group to verify if fully embedded end-bearing piles passing through saturated, loose to medium dense sands and resting on hard layers buckle under the action of axial load alone if the surrounding soil liquefies in an earthquake. During earthquakes, the predominant loads acting on a pile are axial, inertial and lateral movement of the soil (lateral spreading). The failure of a pile can be because of any of these load effects or a suitable combination of them. The centrifuge tests were designed in level ground to avoid the effects of lateral spreading. Twelve piles were tested in a series of four centrifuge tests including some which decoupled the effects of inertia and axial load. The model piles were made of dural alloy tube having an outside diameter of 9.3mm, a thickness of 0.4mm and a total length of 160mm or 180mm. Properties of the model pile can be seen in Bhattacharya et al (2002). The sand used to build the models was Fraction E silica sand, which is quite angular with D_{50} grain size of 0.14mm, maximum and minimum void ratio of 1.014 and 0.613 respectively, and a specific gravity of 2.65. Axial load (P) was applied to the pile through a block of brass fixed at the pile head (Figure 7). With the increase in centrifugal acceleration, the brass weight imposes increasing axial load in the pile. The packages were centrifuged to 50-g and one-dimensional earthquakes were fired and the soil liquefied. The effect of axial load alone was studied by using a specially designed frame to restrain the head mass against inertial action. The frame can be seen later in Figure 10. Table 2 and

Figure 8 summarises the performance of the piles along with the load effects acting. Emphasis is given to the normalised axial load (P/P_{cr}) where P is applied axial load or the axial load at failure. The piles marked 7 and 8 in test SB-04 (Table 2) were tested in similar conditions (in test SB-05, not included in Table 2) but in the absence of soil which simulated Euler’ classical buckling. Thus, through the series of tests the various influences on pile behaviour could be distinguished. Details of all these tests can be seen in Bhattacharya et al (2002, 2003), Bhattacharya (2003).

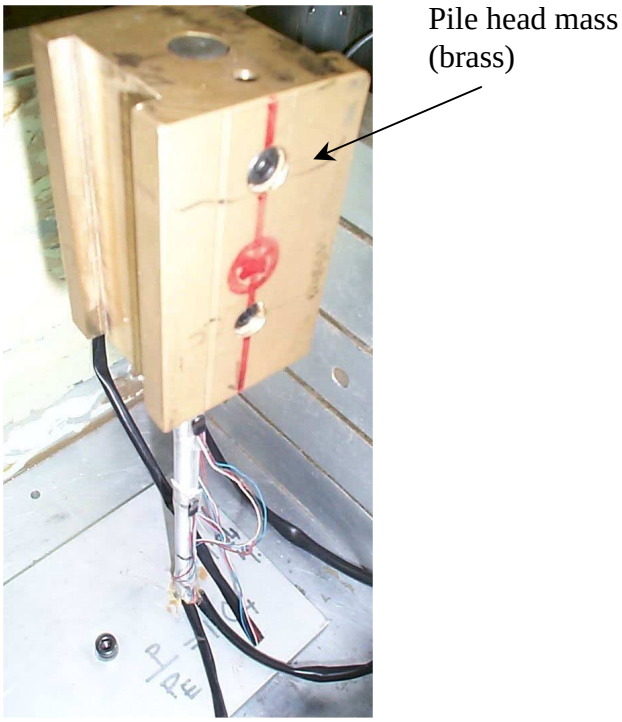

Figure 7: Loading arrangement for Pile 10.

As can be seen from Table 2 and Figure 8, axial load applied to the piles ranged from 22% to 148% of Euler’s elastic critical load (P_{cr}) treating piles as long columns neglecting any support from the soil. From the repeatability of the observations, it immediately becomes obvious from the table that the piles having P/P_{cr} ratio greater than 0.75 failed. This result is consistent with the study of case histories where the piles that failed had (P/P_{cr}) ratio between 0.5 and 1 (see Figure 6).

The loads in the piles marked 7 8 and 10 (see Table 2) were purely axial. The pile heads were restrained in the direction of shaking (no inertia effects) and the piles buckled transversely to the direction of shaking. It must also be remembered that the piles were carrying the same load (load at which it failed) at 50-g and was stable before the earthquake. The stress in the pile section is well within elastic range of the material (less than 30% of the yield strength) but it failed as the earthquake was fired. This confirms that the support offered by the soil was eliminated by

earthquake liquefaction and that the pile started to buckle in the direction of least elastic bending stiffness.

Table 2: Summary of the centrifuge tests

Test ID	**Pile ID**	**Max load (P) N**	**σ =P/A MPa**	**P/P_{cr}**	**Load effects**	**Remarks**	**Reference**
SB-02 Pile length = 160mm; area (A)=9.7 mm^2 Relative Density of the soil = 48%	1	768	79	0.97	Axial + Inertia	Failed	For details see Bhattacharya et al (2002, 2003), Bhattacharya (2003).
	2	642	65	1.01	Axial + Inertia	Failed	
	3	617	63	0.97	Axial + Inertia	Failed	
SB-03 Pile length = 180mm area (A) = 11.2 mm^2 Relative density of the soil = 45%	4	294	26.3	0.5	Axial + Inertia	Did not fail	
	5	220	19.7	0.35	Axial + Inertia	Did not fail	
	6	113	10.1	0.22	Axial + Inertia	Did not fail	
SB-04 Pile length = 180mm; area (A) = 11.2 mm^2 Relative density of the soil = 43%	7	610	54.5	1.04	Axial	Failed	
	8	872	78	1.48	Axial	Failed	
	9	2249	201	0.25	Axial	Did not fail	
SB-06 Pile length = 180mm area (A) = 11.2 mm^2 Relative density of the soil = 40%	10	735	65.6	1.25	Axial	Failed	This paper describes the results of Pile 10.
	11	269	24	0.46	Axial + Inertia	Did not fail	
	12	441	39.4	0.75	Axial + Inertia	Failed	

σ = axial stress in the pile.

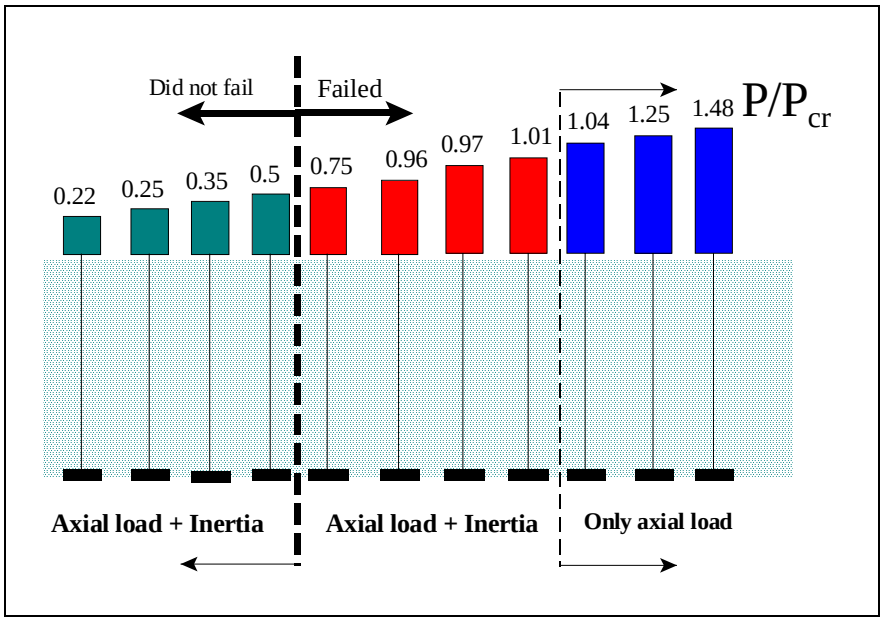

Figure 8: Schematic representation of the test results.

This paper presents the result for pile marked 10 in Table 2. The main aim of the test was to quantify some aspects of pile-soil interaction during seismic liquefaction. Figure 9 shows the instrumentation layout surrounding the pile with an estimate of the pre-existing effective vertical stress (σ_v') at the corresponding elevation. A spring-loaded LVDT was held against the pile head to follow the movement of the pile head. Near field pore pressures were also measured by placing the PPT’s very close to the pile. Miniature earth pressure cells SC2 and SC3 manufactured by Entran were attached to the front and back faces of the pile at 75mm depth (representing 3.75m depth of soil in the prototype scale) to record the pressure changes as the pile buckles. Figure 10 shows the surface observation after the test and Figure 11 reveals the mode shape of pile 10 during excavation. It may be observed that the pile head rotated which is quite similar to the observation of a piled building in the aftermath of a real earthquake.

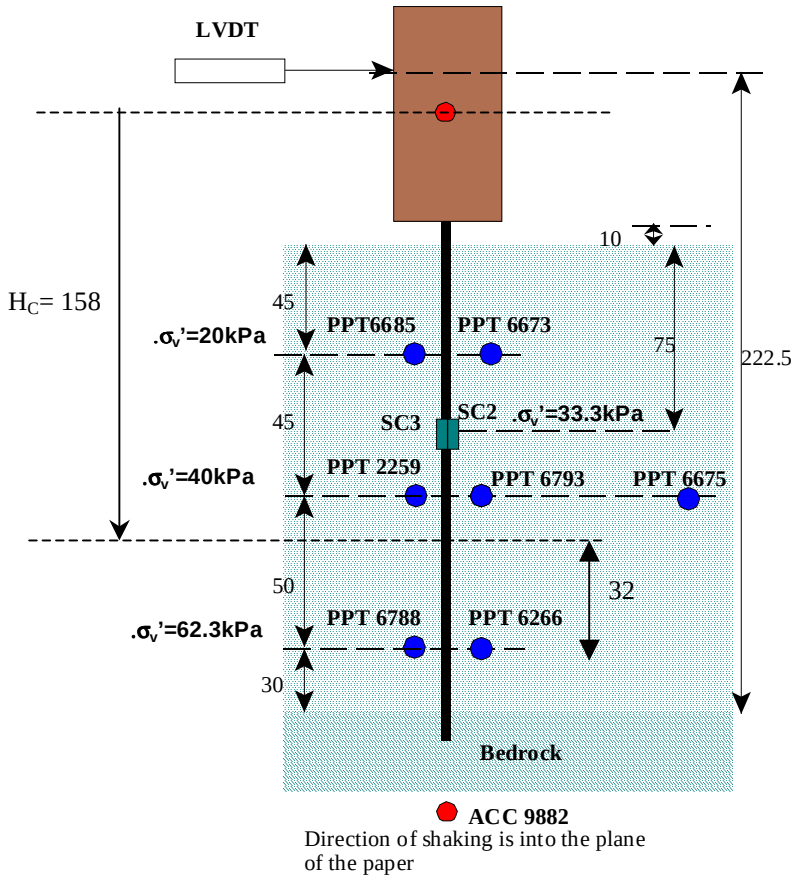

Figure 9: Instrumentation layout surrounding Pile 10 (all dimensions are in mm).

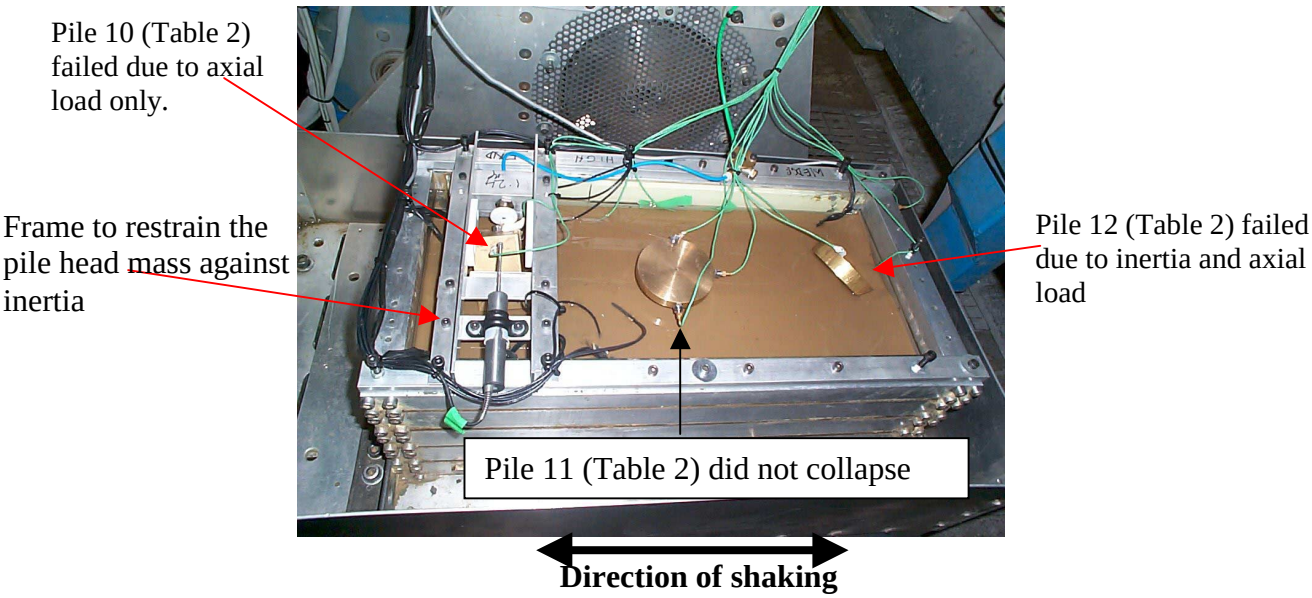

Figure 10: Surface observations after the test SB-06

Figure 11: Mode shape of pile 10 after the test during excavation

Figure 12 plots the time histories of input acceleration, pore pressure records and the LVDT readings. It may be noted that from the PPT records that as shaking starts (0.22s in the time history) pore pressures begin to rise. The LVDT record on the other hand shows that the pile starts to move unidirectionally at around 0.26s in the time history i.e. after two full cycles of loading. It must also be remembered that this unidirectional movement is orthogonal to the direction of shaking and thus denotes the onset of buckling instability. This confirms that the buckling is not linked to inertia. It

must also be noted that the pile begins to buckle when the bottom soil (PPT 6266 in Figure 9) does not liquefy fully (r_u = 82%).

It has been observed through the analysis of pore pressure data in centrifuge tests, Bhattacharya et al (2002, 2003), that as shaking starts the pore pressure rises in the soil starting from the top and proceeding downwards and at the same time, the front of zero effective stress continues to advance swiftly downwards. It has been hypothesised that with the advancement of this front, the pile will gradually be unsupported by the soil grains in a progressive fashion, top-down. When this advancing front reaches a critical depth H_c given by equation 2 (a by- product of Euler's formula), the pile would have become elastically unstable. In Euler's formula $P = \frac{\pi^2}{L_{eff}^2} EI$, taking $L_{eff} = 2H_c$ for a pile with no restraint at the head (Figures 4b and 9), equation 2 is obtained.

$$H_c = \sqrt{\frac{\pi^2 EI}{4P}} \qquad (2)$$

For pile 10, the critical depth (H_c) is estimated to be 158mm from the point of application of the axial load, which is 18mm below the level at which PPT 6675 was placed. Figure 12 shows that PPT 6675, which is 18 mm above H_C has liquefied, but PPT 6266 which is 32mm below H_C has not fully liquefied, when the pile started to buckle.

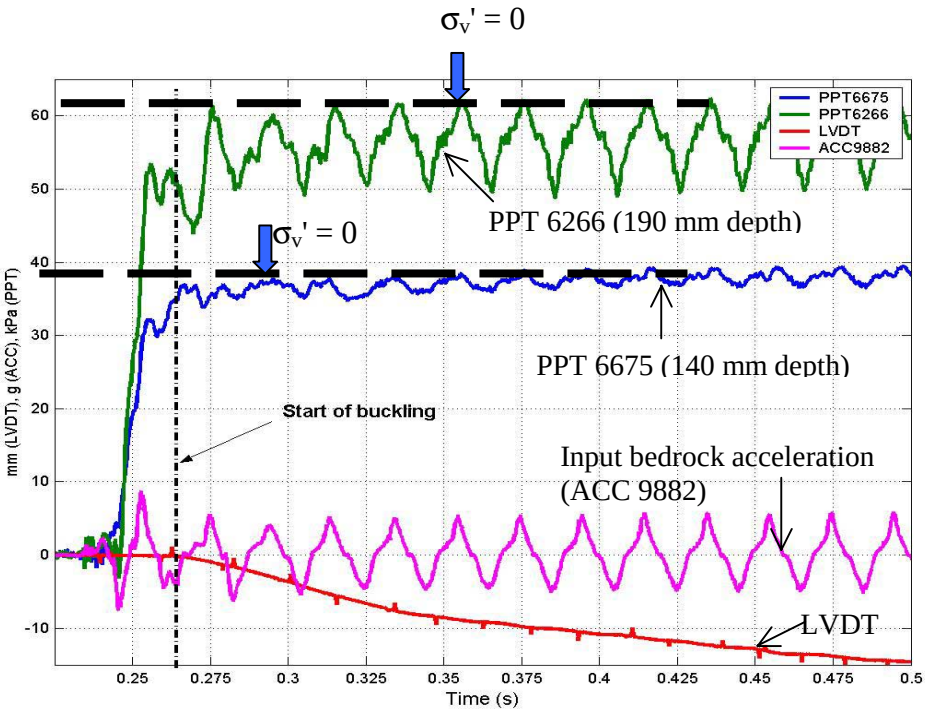

Figure 12: Time histories of input acceleration, pore pressure and LVDT reading for pile 10.

Figure 13 replots the time history of the LVDT record. It can be noted that the gradient of the displacement decreases with the progression of pile movement i.e. buckling. In other words, the pile is having negative acceleration or deceleration and the opposing force must be the resistance of the liquefied soil. In the plot, three parameters are shown in the text boxes for the time intervals at the beginning and end of the buckling of the pile. The values correspond to the level of the pressure cells i.e. at 75mm depth. The parameters are:

1. **Velocity of buckling** (V): It is the rate at which the moving pile loads the soil and it can be linked to the shear strain rate of the neighbouring soil.
2. **Normalised displacement of the pile** (δ/D): δ is the pile displacement and D is the diameter of the pile. It is proportional to the shear strain of the soil. This parameter has been used by Goh and O'Rourke (1999), Takahashi et al. (2002), Haigh (2002).
3. **Normalised velocity of buckling** (V/k) where k is the permeability of the soil. This parameter has been used by Takahashi et al. (2002) to study the lateral resistance of piles in liquefied soil.

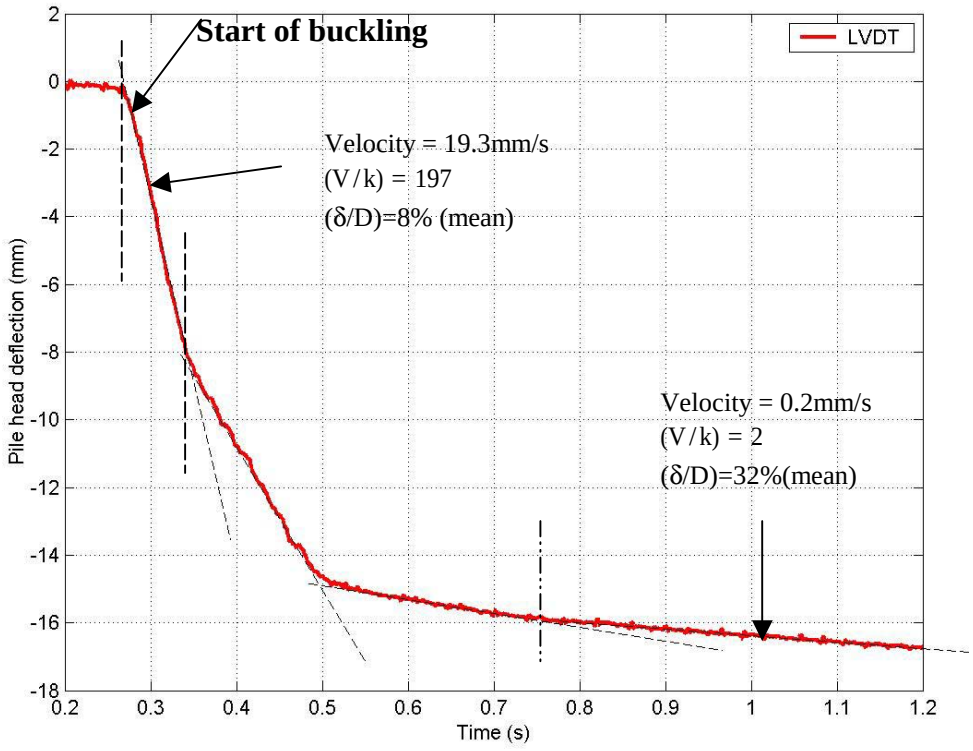

Figure 13: Displacement record of the LVDT in Figure 9

The pile displacement (δ) at the level of the earth pressure cells (i.e. at 75mm depth) is estimated from the LVDT record (which measured the pile head displacement) using a parabolic mode shape

($y = A.x^2$) where A is a function of applied moment. This is essentially the deflection expression of a cantilever beam with moment (M) applied at the free end. It can be justified by the fact that the moment due to the "out of line axial force" is causing the curvature in the pile. Accounting for the soil stiffness will also give a mode shape of second order, but a complicated function of exponential and harmonic, Hetenyi (1946), and is not attempted here. However as the deflection is scaled down proportionally the error would be very marginal. Figure 13 shows that the pile initially moved 8mm without much lateral resistance and then as shearing continues the lateral resistance increases. Other researchers such as Towahata et al. (1999) and Takahashi et al (2002) have reached similar conclusions.

In the experimental work carried out by Takahashi et al (2002) to study the lateral resistance of piles in a liquefied soil, a pile was modelled as a buried cylinder that could be pushed laterally through a liquefied soil having realistic over burden pressure. Pore fluids of different permeability (k) were used in the tests. The displacement rate of the cylinder varied from 1mm/s to 100mm/s. Their test results showed that the initial resistance to movement is negligible at all rates of loading but that some resistance was mobilised after certain amount of displacement. They further conclude that higher the rate of loading the larger is the resistance.

In contrast to the experimental work of Takahashi et al (2002) where a cylinder was pulled at different rates, the failure of the pile discussed here is more realistic. The piles failed due to instability and the rate diminishes from 19.2mm/s to 0.2mm/s, (at the level of pressure cells, see Figure 13) as the pile progressively buckled with the shearing of the soil in front of it. It must be concluded that liquefied soil can generate considerable shear strength if it subjected to undrained monotonic shear strains because of dilative nature.

The difference in the stress cells (SC2 and SC3 in Figure 9) readings approximately measures the lateral resistance offered by the liquefied soil to the buckling pile. The lateral resistance measured is normalised by the initial over burden pressure (33.3kPa) at the level of the pressure cells. Figure 14 shows the plot of normalised lateral resistance with the normalised displacement of the pile (δ/D). It may be noted that lateral resistance increases drastically after 30% of reference strain, which also substantiates the LVDT record. It has been shown by Bhattacharya et al (2002, 2003) that the liquefied soil offers resistance and dictates the hinge formation but cannot prevent the initiation of buckling.

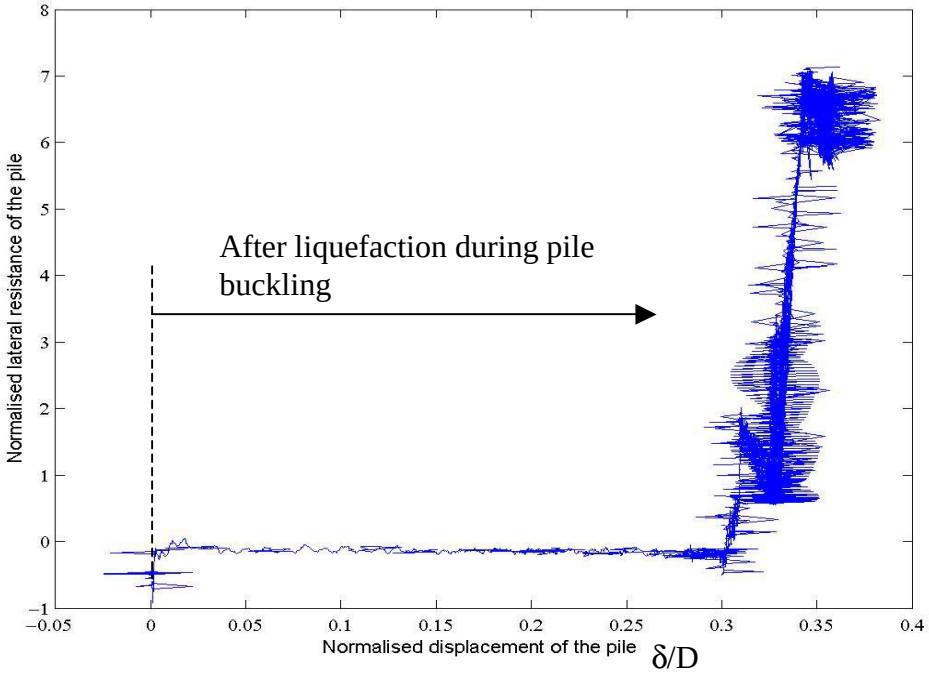

Figure 14: Normalised lateral resistance versus normalised lateral displacement (δ/D).

TRANSIENT LOADING DUE TO LATERAL SPREADING

Dynamic centrifuge model tests have been carried out at Cambridge in which piles with no axial load were placed in laterally spreading slopes, (Haigh, 2002). Instrumentation was in place near to the upslope and downslope faces of these piles in order to measure the lateral total and effective stresses exerted on the piles. Time histories of the differences between the pressures acting on the front and back faces of the pile at the same depth were calculated and showed that significant downslope lateral pressures were exerted on the piles by the laterally spreading ground, as is seen in Figure 15. A summary of the peak lateral stresses measured as acting on the faces of the pile is shown in Figure 16 together with the design loads calculated from the JRA code. The peak stresses at the two depths (2.5 m and 3.25 m) do not occur simultaneously, hence the two lines for maximum loading conditions shown in the figure. It can be seen that the peak applied transient loading exceeds that predicted by the code by a factor of approximately three, whereas post-earthquake residual flow loading is very similar to that predicted by the code.

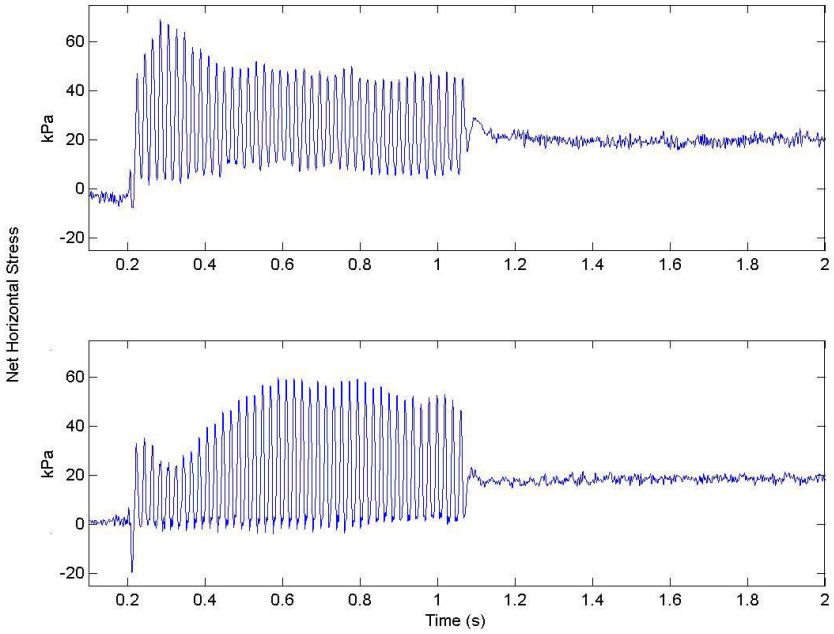

Figure 15: Net downslope total stress acting at 2m and 3.5m depth

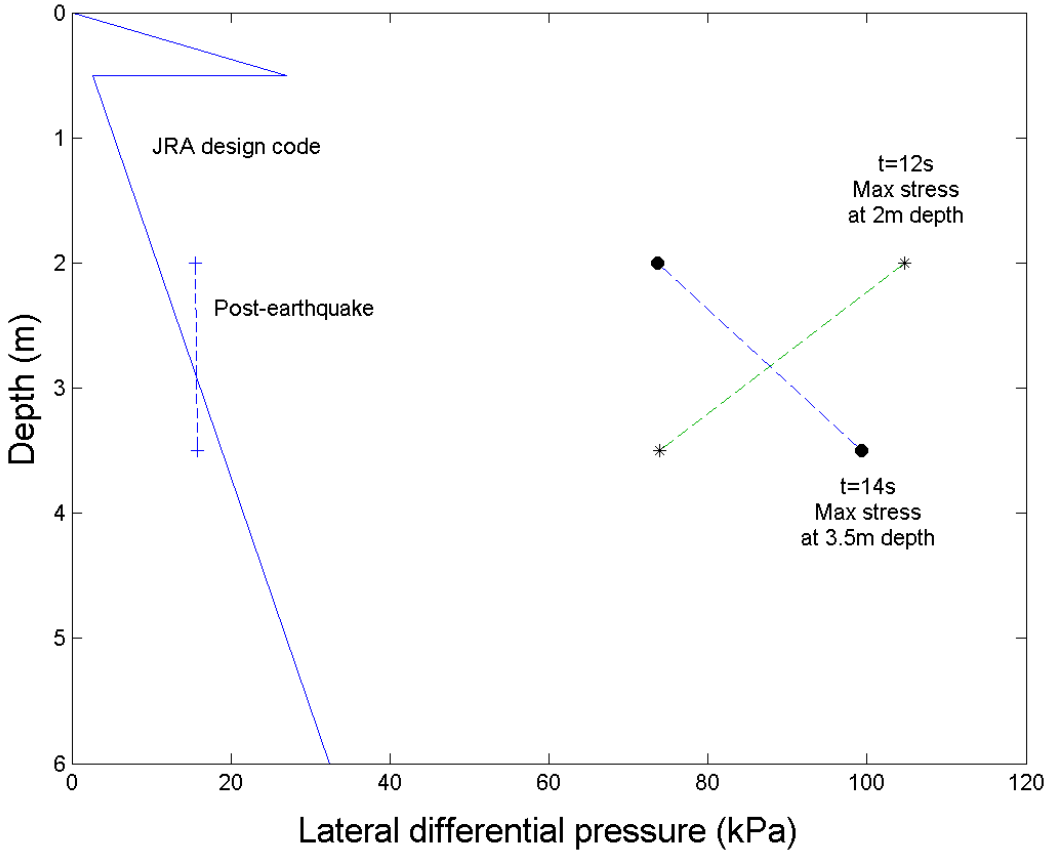

Figure 16: Downslope pressures measured on pile in comparison to those from the JRA code.

PILE–SOIL INTERACTION DURING BUCKLING

Sufficient information has been obtained from the centrifuge tests carried out at University of Cambridge (see Bhattacharya et al 2002, 2003) to propose a hypothesis of pile-soil interaction during a buckling event. The pile begins to buckle when the front of zero effective stress reaches a critical depth H_c. This buckling instability will cause the pile to shear the soil adjacent to it, which will start offering temporary resistance. The soil element in front of the buckling pile will be subjected to monotonic shearing in addition to the cyclic shearing due to earthquake. It is evident from the "V/k" ratio (i.e. the ratio of velocity of the pile to the permeability of the soil, which is 197 at the start, see Figure 13) that the event is best looked upon as undrained. The resistance to the buckling pile is due to this "undrained strength of the soil" which is the strength when sheared at constant volume. It should be obvious from the definition that the stress path must follow the Critical State line, Schofield and Wroth (1968).

It must be expected that the imposition of undrained monotonic shear strain (pile pushing the soil) in loose to medium dense sand at low effective stresses will lead to an attempt to dilate. The event being at constant volume will suppress this potential dilatancy by a negative increment of pore pressure in a locally sheared soil. This negative increment of pore pressure creates an increase in effective stress, which temporarily provides support to the buckling pile. On the other hand, this reduction of pore pressure in the locally sheared soil also induces a transient flow from the neighbouring "liquefied but not monotonically sheared" soil towards the pile. As the far field liquefaction pore pressures are reasserted in the near field, the lateral resistance of the soil to the buckling pile decreases.

A CASE STUDY: FAILURE OF THE SHOWA BRIDGE DURING THE 1964 NIIGATA EARTHQUAKE (JAPAN)

This section describes the bridge and the resulting damage due to the 1964 Niigata earthquake as an example of possible pile failure by buckling. It will be shown that the piles satisfy the criteria of the JRA (1996) code, i.e. had enough strength to resist lateral spreading, but they failed.

The bridge was built over river Shinano and was completed just a month before the earthquake (Fukoka, 1966). The bridge had a width of 24m and total length of 303.9m. The superstructure of the bridge consisted of 12 composite girders. The foundations of each pier consisted of a row of 9 steel tubular piles connected laterally as shown in Figure 17. After the earthquake five girders (G_3 to G_7) fell into the river as shown in Figure 18. Figure 19 shows the post earthquake failure

investigation and recovery of the damaged pile along with the soil investigation data. Table 3 summarises shows the design data of the pile.

Table 3: Design data of pile

Length	25m
External diameter	609mm
Internal diameter	591mm
Material	Steel
E (Young's Modulus)	210GPa

Figure 17: Failure of Showa Bridge.

Eyewitness report

According to a reliable eyewitnesses report, "the girders began to fall somewhat later, perhaps about 0 to 1 minute after the earthquake motion ceased", Hamada, (1992a).

As can be seen from Figure 18, piles of pier no P_5 deformed towards the left and the piles of pier P_6 deformed towards the right (Fukoka, 1966). Had the cause of pile failure been lateral spreading, (Hamada, 1992a) the piers should have deformed identically in the direction of the slope. Furthermore, the piers close to the riverbanks did not fail, whereas here the lateral spread seen to be severe.

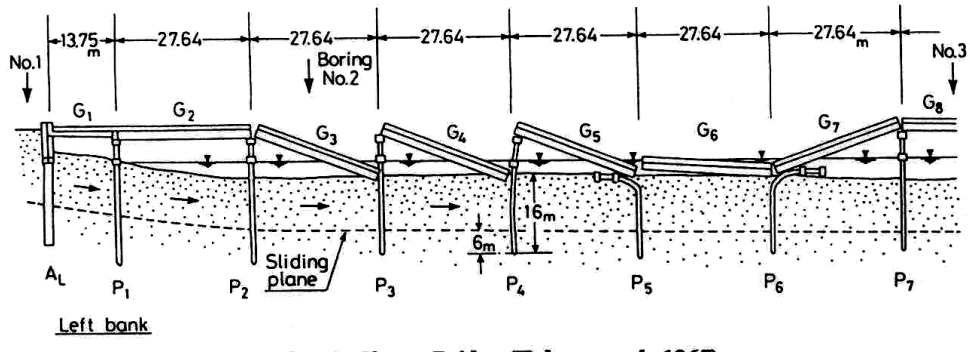

Figure 18: Schematic diagram of the Fall-off of the girders in Showa bridge (Takata et al., 1965)

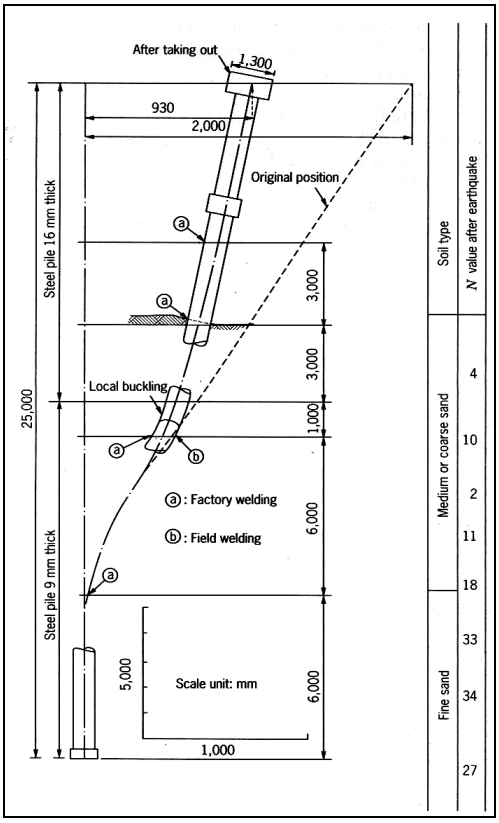

Figure 19: Failed pile and the soil profile, Fukoka (1966).

Bending calculation based on JRA (1996) code

The photographs (Figures 17 and 18) show that the failed piles were fully submerged in water and hence a non-liquefied crust is unlikely to exist. Figure 20 shows the loading diagram based on the JRA code. The calculation below estimates the maximum moment based on JRA code.

Calculations:

Assuming the bulk unit weight of soil is 20kN/m^3,

Maximum lateral spreading pressure at mudline at point A in Figure 20 = 30% of total overburden pressure due to water = $0.3 \times 10\text{kN/m}^3 \times 3\text{m} = 9\text{kPa}$.

Maximum lateral spreading pressure at 10m depth acting at point B in Figure 20 = 30% of total overburden pressure = $0.3 \times (20\text{kN/m}^3 \times 10\text{m} + 10\text{kN/m}^3 \times 3\text{m}) = 69\text{kPa}$.

Maximum moment, at point B in Figure 20, due to spreading force (trapezoidal loading)

= $(0.5 \times 60\ \text{kPa} \times 10\text{m} \times 0.609\text{m} \times 3.33\text{m}) + (9\text{kPa} \times 10\text{m} \times 0.609\text{m} \times 5\text{m}) = 608\text{kNm} + 274\text{kNm} = 882\text{kNm}$.

The plastic moment capacity of the section (9mm thick)

$$= \left(\frac{0.609^3}{6} - \frac{0.591^3}{6} \right) m^3 \times 500MPa = 1620kNm$$

Hence the calculated factor of safety against plastic bending failure= (1620/882)=1.84

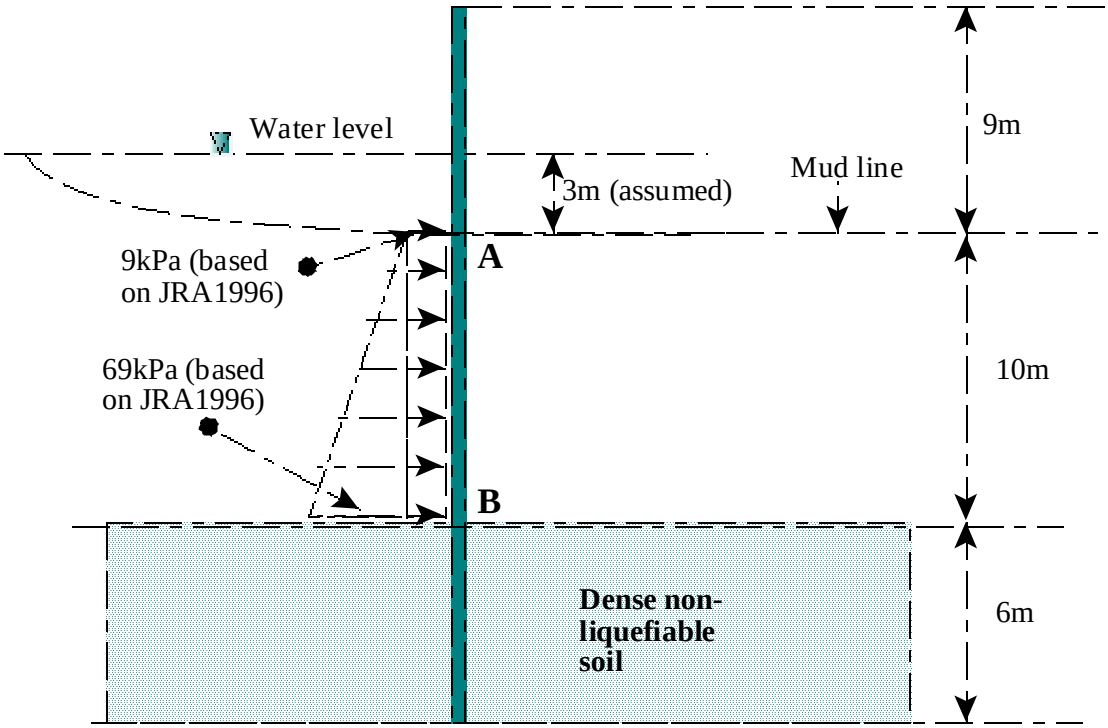

Figure 20: Schematic diagram showing the predicted loading based on JRA code.

Thus, according to the JRA code the bridge should not have collapsed. In addition the hinge formed at 4 m below the mud line (as can be seen from Figure 19) whereas the moment should be a maximum at 10m depth based on JRA code and should be only 5% of the plastic moment of resistance at the location of the observed hinge.

Simple buckling calculation

For the Showa Bridge piles, the estimated allowable load is 965 kN and the theoretical buckling load, P_{cr} (assuming liquefied soil did not offer support) is 1095kN i.e. only 15% greater than the allowable load. The calculations are shown below.

CONVENTIONAL PILE CAPACITY:

The pile capacity is estimated based on SPT values quoted in Figure 19. Standard correlations, Randolph (1985) have been used and the values are shown in Figure 21. It has been assumed that the design axial load of the pile is quite close to the allowable load.

Shaft resistance

Layer 1 (outer) = $\pi \times 0.609\text{m} \times 10\text{m} \times 30\text{kPa} = 573\text{kN}$

Layer 2 (outer) = $\pi \times 0.609\text{m} \times 6\text{m} \times 50\text{kPa} = 573\text{kN}$

Base resistance

Plugged mechanism = $\pi/4 \times (0.609)^2 m^2 \times 7500kPa = 2184kN$

Unplugged mechanism = $\pi/4 \times [(0.609)^2 - (0.591)^2] m^2 \times 7500kPa = 127kN$

ULTIMATE PILE CAPACITY

Plugged mechanism = (573 + 573 + 2184) kN = 3300 kN

Unplugged mechanism = [(573 +573) × 2 + 127] kN = 2419 kN

P = ALLOWABLE LOAD IN PILE (using a factor of safety of 2.5)= 2419/2.5 = 965 kN

Length of the pile in liquefiable zone is10m and the length of pile in free air/water is 9m. Thus pile in unsupported zone during liquefaction is 19m. From the buckled shape (shown as original position in Figure 19, it is clear that the pile had fixed-free boundary condition and hence the effective length is twice the length in unsupported zone. It is also in some way similar to the shape as observed in Figure 3.

STRUCTURAL PROPERTIES OF PILE:

Moment of inertia of the pile (I) = $\frac{\pi}{64}\left(0.609^4 - 0.591^4\right)m^4 = 7.63\times10^{-4} m^4$

Effective length of pile (L_{eff}) = 2 × 19m = 38m

BUCKLING LOAD OF PILE (P_{cr})

= $\frac{\pi^2}{L_{eff}^2} EI = \frac{\pi^2}{38^2 m^2} \times 210GPa \times 7.63\times10^{-4} m^4 = 1095kN$

Structural engineers generally demand a load factor of at least 3 against linear elastic buckling to allow for eccentricities and reduction of stiffness due to yielding. Thus, to avoid buckling instability the applied load should not have exceeded (1095/3) kN = 365kN.

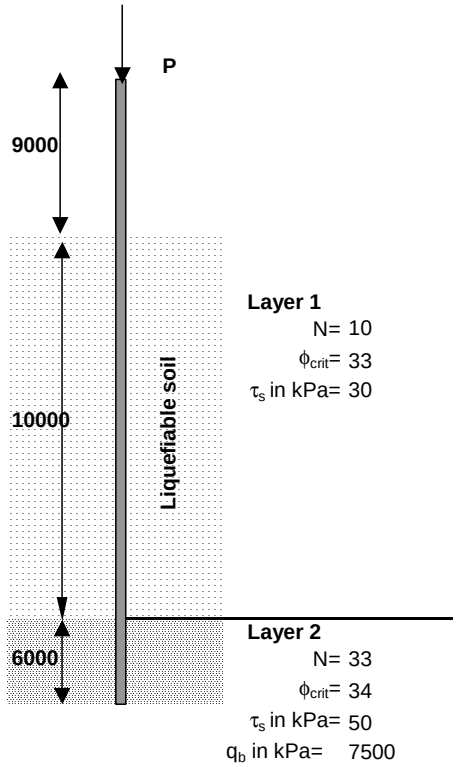

Figure 21: Design data to estimate the conventional pile capacity.

ACTUAL AXIAL LOAD AT FAILURE

This section calculates the dead load on each pile from the configuration of the Showa Bridge deck. Information of the dimensions of the girders, span and the bridge type is obtained from Iwasaki (1984). Reasonable assumptions are made for the missing data. A schematic diagram of the deck is shown in Figure 22.

The bridge has a total length of 303.9 m (13.75 m + 10@ 27.64 m + 13.75 m) and width of 24 m. As mentioned earlier, the superstructure of the bridge consists of 12 composite steel simple span girders. There are 9 piles in a row sharing the load of the superstructure (see Figure 17). Table 4 shows the estimate of the total dead load for each span. It is assumed in the analysis that the load of the deck is shared equally by each of the 9 piles.

It is very interesting to note that the dead load per pile is in the order of 740 kN. If the live load due to the vehicular loading is added, the total load will be near 1000 kN. The allowable load predicted based on the soil parameter (N values) is 965kN, which justifies the assumption that the design load of the pile is close to the allowable load.

Table 4: Dead load calculation for Showa Bridge

Item	**Details**	**Load**
Slab and asphalt top	24.8m×27.64m×(0.2+0.05) m ×25kN/m^3	4146kN
Crash barrier	2×1.5m×0.1m×27.64×25kN/m^3	207.3kN
Kerb	2m×0.15m×27.64m×25kN/m^3	207kN
9 steel girders	27.64m×9×5.2kN/m	1294kN
Stiffeners, bolts	30% of girder weight	388kN
Bottom Girder	0.7m×1.0m×24m×25kN/m^3	420kN
Total		6662kN
Load per pile = 6662kN/9		**740kN**

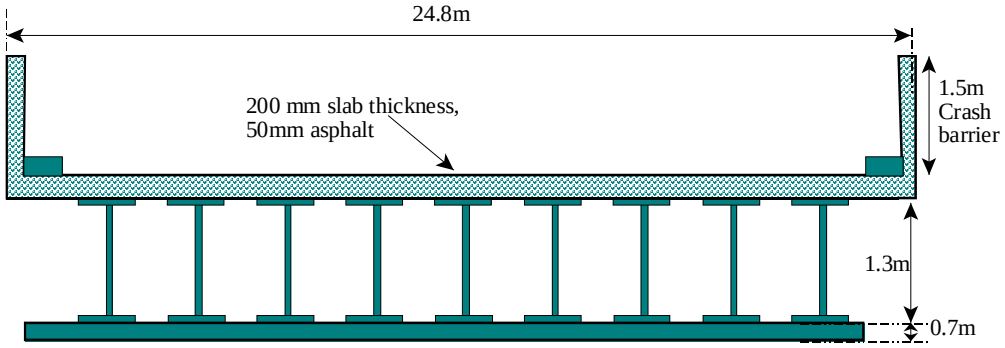

Figure 22: Schematic of the Showa Bridge deck (adapted from Iwasaki, 1984)

DISCUSSION

Distinguishing between buckling and bending

In design, beam bending and column buckling are approached in two different ways. Piles have erroneously been designed as cantilever beams. Bending is a stable mechanism, i.e. if the lateral load is withdrawn, the pile comes back to its initial configuration provided the yield limit of the material has not been exceeded. This failure mode depends on the bending strength (moment for first yield, M_Y; or plastic moment capacity, M_P) of the member under consideration. On the other hand, buckling is an unstable mechanism. It is sudden and occurs when the elastic critical load is reached. It is the most destructive mode of failure and depends on the geometrical properties of the member, i.e. slenderness ratio and not on the yield strength of the material.

For example, steel pipe piles having identical length and diameter but having different yield strength [f_y of 200MPa, 500MPa, 1000MPa] will buckle at almost the same axial load but can resist

different amounts of bending. Bending failure may be avoided by increasing the yield strength of the material, i.e. by using high-grade concrete or additional reinforcements, but it may not suffice to avoid buckling. To avoid buckling, there should be a minimum pile diameter depending on the depth of the liquefiable soil.

The JRA code was formulated by back analysing piled foundations, which were not seriously damaged. It is worth noting that the foundation piles had a diameter of 1.5m and penetrated only 15.9m of length in liquefied layer, Yokoyama et al., (1997). The slenderness ratio in the liquefiable region is thus 42 and they could be categorised as short columns, which would only fail in crushing and not buckling. Such piles would remain stable irrespective of soil support, but they would need to be checked against bending moment induced due to lateral spreading.

Possible mechanism of failure of the Showa Bridge.

Earthquake-induced shaking caused the pore pressures to build up in the loose saturated sandy soil, and the soil started to liquefy. The piles lost their shaft resistance in the liquefiable region (layer 1 in Figure 21) and transferred the loads downwards to layer 2 with minor settlements. The soil liquefied and therefore lost its stiffness causing the pile to act temporarily as an unsupported column. The pile became elastically unstable and began to move sideways in the direction of least elastic stiffness, shearing the soil next to it. The initial resistance to the movement of the pile offered by the liquefied soil will be negligible but a large undrained shear resistance can be mobilised after a certain amount of monotonic displacement. The undrained resistance of initially liquefied soil is caused by negative excess pore water pressures, due to suppressed dilation, in the shear zone and depends on the velocity of buckling as observed by Takahashi et al. (2002) and discussed in the earlier section of the paper. This dilatant sand can hold a buckling pile in quasi-static equilibrium.

The pore pressure difference between the shear zone and the liquefied far field causes a transient flow towards the pile. As the pore pressure in the shear zone increases again, its lateral resistance reduces. The pile is now displaced out of the initial straight line and cannot move back to equilibrium position. In other words the movement is unidirectional.

It is the upper part of a liquefiable sand layer that remains longest in a state of liquefaction ($\sigma_v'=0$) due to upward hydraulic gradients, and it is the upper part of the pile which displaces most, and which can fully soften the supporting soil adjacent to it. The imbalance between reducing soil support, increasing bending moment created by lateral displacement of the pile cap (out of line vertical force), and deteriorating bending stiffness of the pile, inevitably leads to the formation of a

relatively shallow plastic hinge. The proposed mechanism of softening due to transient flow may explain the delay of a few minutes in the pile failure

Improvement suggested for the JRA code in the light of observed seismic pile failures and back analysis.

It has been demonstrated in the earlier section of the paper that buckling is a possible failure mode of piled foundations. Lateral loading due to slope movement, inertia or out-of-line straightness increases lateral deflections, which in turn reduces the buckling load. These lateral loads are, however, secondary to the basic requirements that piles in liquefiable soils must be checked against Euler's buckling. In contrast, the current method of pile design under earthquake loading is based on a bending mechanism where the inertia or slope movement (lateral spreading of soil) induce bending moments in the pile, and where axial load effects are ignored. The JRA code is inadequate and buckling needs to be addressed. Other codes such as NEHRP (2000) or Eurocode 8 (1998) also omits consideration necessary to avoid buckling of piles due to loss of soil support in the event of soil liquefaction.

Stability analysis of elastic columns shows (Timoshenko and Gere, 1961) that lateral deflections caused by lateral loads are greatly amplified if the axial load approaches the elastic critical load P_{cr}. In the presence of an axial load of magnitude 65% of P_{cr}, the sway deflections and bending strains will be 3 times those of small deflection theory. In most practical situations such enhanced strains also lead to degradation of the elastic stiffness of the column, bringing down the critical load and causing collapse. It can be shown that a slenderness ratio of 50 signifies (P/P_{cr}) below 0.35 for steel and 0.15 for concrete, Bhattacharya (2003). In each case, the expected amplification due to the combined action of lateral and axial loads is negligible. This suggests that for piles having slenderness ratio below 50, lateral loads – if properly accounted for in simple bending calculations - cannot lead a pile to fail prematurely. This is also consistent with the fact that piles in laterally spreading soil (Marked A through F in Figure 5) having slenderness ratio below 50 did not collapse. It is proposed in this paper that piles in liquefiable soil should be maintained below a slenderness ratio of 50 to avoid buckling instability.

CONCLUSIONS

1. Buckling is a possible failure mechanism of piled foundations in areas of seismic liquefaction. Lateral loading due to slope movement, inertia or out-of-line straightness reduces the buckling load and promotes more rapid collapse. These lateral load effects are, however, secondary to the basic requirements that piles in liquefiable soils must be checked

against Euler’s buckling. In contrast, the current codes of practice for pile design omit considerations necessary to avoid buckling in event of soil liquefaction. These codes are inadequate and buckling needs to be addressed. It is proposed in this paper that piles in liquefiable soil should be maintained below a slenderness ratio of 50 to avoid buckling instability. The main difference between the proposed mechanism of pile failure and instability of structural frame shown in Figure 3 is that the soil offering resistance to the buckling pile. The buckling of piles in liquefiable soils can be described as the buckling of slender columns in a non-linear resistive medium. The resistance is due to the dilating, “initially liquefied and then subsequently monotonically sheared” near field soil. Figure 23 shows a very simple conceptual model of pile failure in level ground.

2. Bending and buckling require different approaches in design. Bending is a stable mechanism and is dependent on strength whereas buckling is dependent on geometric stiffness and is almost independent of strength. Designing against bending would not automatically suffice the buckling requirements. Thus, there is a need to reconsider the safety of existing piled foundations in potentially liquefiable soils designed based on the current codes of practice.

3. Centrifuge tests were designed in level grounds to avoid the effects of lateral spreading and the test results verified the hypothesis of pile failure due to buckling instability. The key parameter identified to distinguish whether the pile pushes the soil (buckling) or the soil pushes the pile (lateral spreading) is the slenderness ratio of the pile in the liquefiable region. The critical value of this parameter is approximately 50.

4. Liquefied soil cannot prevent the initiation of buckling but will dictate the location of a hinge by offering lateral resistance to the buckling pile. The quantification of lateral resistance is dependent of various factors. However, from the design point of view, the quantification of lateral resistance is irrelevant because of the fact that piled structure should not become unstable even at full liquefaction.

5. Future research development and regulations for piled foundations should focus on two issues:
    - Retrofitting measures for existing piled foundations subject to buckling.

- Promulgation of new codes of practice to forbid unprotected slender piles and encourage the use of fewer high modulus piles, and cellular arrangements.

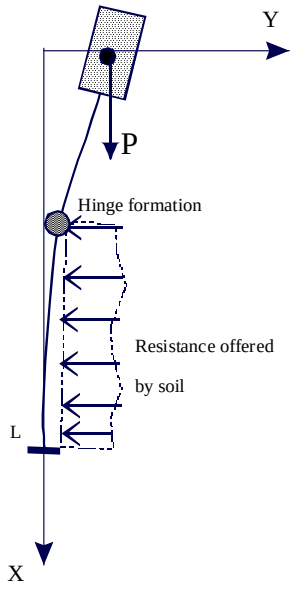

Figure 23: Conceptual model of pile failure in level ground.

REFERENCES

1. Abdoun, T and Dobry, R (2002). "Evaluation of pile foundation response to lateral spreading", Soil Dynamics and Earthquake Engineering., No 22, pp. 1051-1058.
2. Berrill, J.B., Christensen, S. A., Keenan, R. P., Okada, W. and Pettinga, J.R. (2001): Case Studies of Lateral Spreading Forces on a Piled Foundation. *Geotechnique* **51**, No. 6, pp 501-517.
3. Bhattacharya, S and Bolton, M.D (2004a), "A fundamental omission in seismic pile design leading to collapse", Proc. of the 11th International Conference on Soil Dynamics and Earthquake Engineering, 7-9th Jan 2004, Berkeley.
4. Bhattacharya, S and Bolton, M.D (2004b), "Errors in design leading to pile failure during seismic liquefaction", Proc. of the 5th International Conference on Case Histories in Geotechnical Engineering, New York, 13-17th April 2004.
5. Bhattacharya, S [2003]. "Pile Instability during earthquake liquefaction", PhD Thesis, University of Cambridge (U.K).
6. Bhattacharya S, Madabhushi S.P.G and Bolton M.D [2003]. "Pile Instability during earthquake liquefaction", *Proc. of the 16th ASCE Engineering Mechanics Conference (EM-03)*, Paper no 404, University of Washington, Seattle, 16-18th July 2003.
7. Bhattacharya, S (2002): Analysis of reported case histories of pile foundation performance during earthquakes, *Proceedings of 7th British Geotechnical Association (BGA) Young Geotechnical Engineers Symposium, Dundee*, 17th to 19th July 2002.
8. Bhattacharya, S., Madabhushi, S.P.G and Bolton, M.D (2002): An alternative mechanism of pile failure in liquefiable deposits during earthquakes, *Technical report of University of Cambridge, CUED/D-SOILS/TR324* (Oct 2002). This has been accepted for publication in Geotechnique. It can be seen at http://www-civ.eng.cam.ac.uk/geotech_new/publications/TR/TR324.pdf

9. Eurocode 8: Part 5 [1998]. Design provisions for earthquake resistance of structures-foundations, retaining structures and geotechnical aspects, European Committee for standardization, Brussels
10. Fleming, W.G.K., Weltman, A.J., Randolph, M.F. and Elson, W.K [1992]. "*Piling Engineering*". Second edition, John Wiley & Sons.
11. Finn L.W.D and Thavaraj, T (2001): Deep Foundations in Liquefiable Soils: Case Histories, Centrifuge Tests and Methods of Analysis. *Proceedings: Fourth International Conference on Recent Advances in Geotechnical Earthquake Engineering and Soil Dynamics and Symposium in honour of Professor W.D.Liam Finn* San Diego, California, March 26-31, 2001.
12. Finn, W.D.L and Fujita, N [2002]. "Piles in liquefiable soils: seismic analysis and design issues", Soil Dynamics and Earthquake Engineering., No 22, pp 731-742
13. Fukoka, M (1966). Damage to Civil Engineering Structures, *Soils and Foundations*, Tokyo, Japan, Volume-**6** (2), March 1966, pp 45-52.
14. Goh, S and Rourke T.D (1999). Limit state model for soil-pile interaction during lateral spread. *Proc. 7th. U.S.-Japan Workshop on Earthquake Resistant Design of lifeline facilities and countermeasures against soil liquefaction. Seattle, WA.*
15. Haigh, S.K (2002): Effect of earthquake-induced liquefaction on piled foundations in sloping ground. *PhD thesis*. Cambridge University Engineering Department (U.K).
16. Hamada, M [2000]. "Performances of foundations against liquefaction-induced permanent ground displacements", Paper 1754, *Proc. of the 12th World Conference on earthquake engineering*, Auckland, New Zealand.
17. Hamada, M. (1992a). Large ground deformations and their effects on lifelines: 1964 Niigata earthquake. *Case Studies of liquefaction and lifelines performance during past earthquake. Technical Report NCEER-92-0001, Volume-1, Japanese case studies, National Centre for Earthquake Engineering Research.* Buffalo, NY.
18. Hamada, M. (1992b). Large ground deformations and their effects on lifelines: 1983 Nihonkai-Chubu earthquake. *Case Studies of liquefaction and lifelines performance during past earthquake. Technical Report NCEER-92-0001, Volume-1, Japanese case studies, National Centre for Earthquake Engineering Research.* Buffalo, NY.
19. Hetenyi, M (1946): "Beams on elastic foundations", The University of Michigan Press.
20. IS-1893 (2002): Criteria for earthquake resistant design. Bureau of Indian Standard (BIS). New Delhi, India.
21. Ishihara, K. (1997). Terzaghi oration: Geotechnical aspects of the 1995 Kobe earthquake. *Proceedings of ICSMFE*. Hamburg, pp 2047-2073.
22. Ishihara, K [1993]. Rankine lecture- "Liquefaction and flow failure during earthquakes", Geotechnique 43, No 3, pp 351-415.
23. JRA (1996). Japanese Road Association, *Specification for Highway Bridges, Part V, Seismic Design.*
24. National Research Council (NRC, 1985): Liquefaction of soils during earthquakes. Washington, DC: *National Academic Press*.
25. National Earthquake Hazards Reduction Program (NEHRP) [2000]. Commentary (Federal Emergency Management Agency, USA, 369) for seismic regulations for new buildings and other structures.
26. Ramos, R., Abdoun, T.H., Dobry, R (2000): "Effects of lateral stiffness of superstructure on bending moments of pile foundation due to liquefaction induced lateral spreading", Proceedings of the 12th World Conference on Earthquake Engineering, Auckland, New Zealand.
27. Randolph, M.F (1985): "Capacity of piles driven into dense sand". *Technical Report of Cambridge University*. CUED/D-SOILS TR 171.

28. Sato, M., Ogasawara, M. and Tazoh, T. (2001): "Reproduction of Lateral Ground Displacements and Lateral-Flow Earth Pressures Acting on a Pile Foundations Using Centrifuge Modelling". *Proceedings: Fourth International Conference on Recent Advances in Geotechnical Earthquake Engineering and Soil Dynamics and Symposium in Honor of Professor W.D.Liam Finn*. San Diego, California, March 26-31, 2001.
29. Schofield, A.N and Wroth, C.P (1968). "Critical State Soil Mechanics", McGraw-Hill, London.
30. Soga, K. (1997). Chapter 8, "Geotechnical aspects of Kobe earthquake", of *EEFIT report*, Institution of Structural Engineers, *UK*.
31. Takahashi, A., Kuwano, Y., and Yano, A. (2002). Lateral resistance of buried cylinder in liquefied sand. *Proceedings of the International Conference on physical modelling in geotechnics, ICPMG-02*. St. John's, Newfoundland, Canada, 10-12th July.
32. Takata, T., Tada, Y., Toshida, I. and Kuribayashi, E. (1965). Damage to bridges in Niigata earthquake. *Report no-125-5*, Public Works Research Institute (in Japanese).
33. Timoshenko, S.P and Gere, J.M [1961]. "*Theory of elastic stability*", McGraw-Hill Book company, New York.
34. Tokimatsu, K., Suzuki, H and Suzuki, Y (2001) Back-calculated p-y relation of liquefied soils from large shaking table tests, Proceedings: Fourth International Conference on Recent Advances in Geotechnical Earthquake Engineering and Soil Dynamics and Symposium in honour of Professor W.D.Liam Finn San Diego, California, March 26-31, 2001.
35. Tokimatsu K., Oh-oka Hiroshi, Satake, K., Shamoto Y. and Asaka Y. (1998). Effects of Lateral ground movements on failure patterns of piles in the 1995 Hyogoken-Nambu earthquake. *Proceedings of a speciality conference, Geotechnical Earthquake Engineering and Soil Dynamics III, ASCE Geotechnical Special publication* No **75**, pp 1175-1186.
36. Tokimatsu K, Mizuno H. and Kakurai M. (1996). Building Damage associated with Geotechnical problems. Special issue of *Soils and Foundations*, Japanese Geotechnical Society, Jan 1996, pp 219-234.
37. Yokoyama, K., Tamura, K and Matsuo, O (1997): *Design methods of bridge foundations against soil liquefaction and liquefaction-induced ground flow*. Second Italy-Japan workshop on seismic design and retrofit of bridges, Rome, Italy, Feb 27 and 28, 1997.
38. Towahata, I., Vargas-Mongem, W., Orense, R.P and Yao, M (1999): "Shaking table tests on subgrade reaction of pipe embedded in sandy liquefied subsoil", Soil Dynamics and Earthquake Engineering, Vol 18, No 5, pp 347-361.